The Astrophysical Journal, 680:728–733, 2008 June 10

CHARA ARRAY MEASUREMENTS OF THE ANGULAR DIAMETERS OF EXOPLANET HOST STARS

Ellyn K. Baines,[1] Harold A. McAlister, Theo A. ten Brummelaar, Nils H. Turner, Judit Sturmann, Laszlo Sturmann, and P. J. Goldfinger
Center for High Angular Resolution Astronomy, Georgia State University, P.O. Box 3969, Atlanta, GA 30302-3969; baines@chara.gsu.edu, hal@chara.gsu.edu, theo@chara-array.org, nils@chara-array.org, sturmann@chara-array.org, pj@chara-array.org

and

Stephen T. Ridgway
Kitt Peak National Observatory, National Optical Astronomy Observatory, P.O. Box 26732, Tucson, AZ 85726-6732; ridgway@noao.edu
Received 2007 November 2; accepted 2008 March 3

ABSTRACT

We have measured the angular diameters for a sample of 24 exoplanet host stars using Georgia State University's CHARA Array interferometer. We use these improved angular diameters together with *Hipparcos* parallax measurements to derive linear radii and to estimate the stars' evolutionary states.

Subject headings: infrared: stars — planetary systems — stars: fundamental parameters — techniques: interferometric

Online material: extended figure, machine-readable table

1. INTRODUCTION

Nearly 300 exoplanet systems are now known, discovered via radial velocity surveys and photometric transit events. Most known exoplanet host stars are Sun-like in nature, and their planets have minimum masses comparable to Saturn, with orbital semimajor axes ranging from 0.04 to 6.0 AU (Marcy et al. 2005), painting pictures of planetary systems very different from our own.

Many exoplanet host stars' angular diameters have been estimated using photometric or spectroscopic methods. For example, Ribas et al. (2003) matched 2MASS infrared photometry to synthetic photometry in order to estimate stellar temperatures, which then produced angular diameter estimations. Fischer & Valenti (2005) performed the first uniform spectroscopic analysis for all the exoplanets' host stars known at the time, as well as for a large sample of single stars. They determined the effective temperature $T_{\rm eff}$, $\log g$, $v \sin i$, and metallicity for 1040 FGK-type stars to check whether there were any correlations between stellar metallicity and the presence of planets, and found a rapid rise in the fraction of stars with planets for high-metallicity stars. They calculated stellar radii using stellar luminosities derived from $T_{\rm eff}$, *Hipparcos* parallaxes, and a bolometric correction.

These methods are useful for estimating stellar sizes, but are inherently indirect in nature. Interferometric observations directly measure the angular diameters for these stars, which, in conjunction with parallaxes, lead to linear radii.

2. INTERFEROMETRIC OBSERVATIONS

The target list was derived from the general exoplanet list using declination limits (north of -10°) and magnitude constraints. The stars needed to be brighter than $V = +10$ in order for the tip/tilt subsystem to lock onto the star, and brighter than $K = +6.5$ so that fringes were easily visible. This reduced the exoplanet list to approximately 80 targets, and we obtained data on 24 of them over multiple observing runs spanning 2004 January to 2007 September (see Table 1).

The stars were observed using the Center for High Angular Resolution Astronomy (CHARA) Array, a six-element Y-shaped interferometric array located on Mount Wilson, California (ten Brummelaar et al. 2005). The Array currently employs visible wavelengths (470–800 nm) for tracking and tip/tilt corrections, and near-infrared bands (H at 1.67 μm and K' at 2.15 μm) for fringe detection and data collection. All observations were obtained using the pupil-plane "CHARA Classic" beam combiner in the K' band, except observations of HD 189733, which were obtained using the H band. The observing procedure and data-reduction process employed here are described in McAlister et al. (2005).

Most observations were taken using the longest baseline the CHARA Array offers, 331 m for the S1-E1 pair of telescopes, due to its sensitivity in measuring stellar diameters.[2] If no S1-E1 data were obtained, the observations with the longest available baseline were used in the angular diameter measurement. Table 1 lists the exoplanet host stars observed, their calibrators, the baseline used, the dates of the observations, and the number of observations obtained. More information on the transiting planet system HD 189733 can be found in Baines et al. (2007).

We used the standard calibrator-target-calibrator observing pattern, so that every target was flanked by calibrator observations made as close in time as possible. This allowed us to calculate the target's calibrated visibilities from the raw visibilities of the target and calibrator. Acceptable calibrators were chosen to have expected visibility amplitudes greater than 85% on the baselines used, and the high visibilities meant that the calibrators were nearly unresolved. Therefore, uncertainties in the calibrator's diameter do not affect the target's diameter calculation as much as if the calibrator star had a significant angular size on the sky.

Another small source of potential systematic error in the target's diameter measurement arises from limb-darkening effects, although the error is on the order of a few percent and is not as significant an effect in the K' band as it would be for measurements

[1] For reprints, please email baines@chara.gsu.edu.

[2] The three arms of the Array are denoted by their cardinal directions: "S" is south, "E" is east, and "W" is west. Each arm bears two telescopes, numbered "1" for the telescope farthest from the beam combining laboratory and "2" for the telescope closer to the laboratory.

TABLE 1
Observing Log

Target HD	Other Name	Calibrator HD	Baseline (length)	Date (UT)	Number of Observations
3651	54 Psc	4568	S1-E1 (331 m)	2005 Oct 22	2
				2005 Oct 24	6
9826	υ And	6920	S1-E1 (331 m)	2004 Jan 14	13
				2004 Jan 15	6
			W1-S2 (249 m)	2007 Sep 05	15
10697	109 Psc	10477	S1-E1 (331 m)	2005 Oct 23	4
				2007 Sep 13	2
				2007 Sep 14	4
11964	...	13456	W1-S1 (279 m)	2005 Dec 13	1
				2005 Dec 16	5
13189	...	11007	S1-E1 (331 m)	2005 Dec 12	4
				2006 Aug 14	4
19994	94 Cet	19411	S1-E1 (331 m)	2005 Oct 21	4
				2005 Oct 27	6
				2005 Dec 10	6
20367	...	21864	S1-E1 (331 m)	2005 Dec 12	5
				2007 Jan 24	2
23596	...	22521	S1-E1 (331 m)	2007 Sep 11	7
				2007 Sep 14	5
38529	...	43318	S1-E1 (331 m)	2005 Oct 22	2
				2005 Oct 24	2
				2005 Dec 06	8
50554	...	49736	S1-E1 (331 m)	2005 Dec 07	2
				2005 Dec 12	5
59686	...	61630	S1-E1 (331 m)	2005 Dec 06	8
				2007 Apr 02	9
75732	55 Cnc	72779	S1-E1 (331 m)	2007 Mar 26	5
				2007 Mar 30	6
104985	...	97619	E1-W1 (314 m)	2007 Apr 26	7
117176	70 Vir	121107	S1-E1 (331 m)	2006 May 20	5
				2007 Apr 02	6
120136	τ Boo	121107	S1-E1 (331 m)	2007 Feb 05	10
				2007 Mar 25	2
				2007 Mar 26	5
				2007 Mar 30	8
143761	ρ CrB	136849	S1-E1 (331 m)	2006 May 19	4
				2006 Jun 09	1
145675	14 Her	151044	S1-E1 (331 m)	2006 Aug 11	3
				2006 Aug 12	7
177830	...	176377	S1-E1 (331 m)	2006 Jun 09	1
				2006 Aug 13	6
186427	16 Cyg B	184960	S1-E1 (331 m)	2006 Aug 13	6
				2007 Sep 12	6
189733	...	190993	S1-E1 (331 m)	2006 May 31	1
				2006 Jun 01	2
				2006 Jun 08	1
				2006 Aug 15	5
190228	...	190470	S1-E1 (331 m)	2006 Aug 14	8
190360	...	189108	S1-E1 (331 m)	2006 Jun 09	1
				2006 Aug 11	9
196885	...	194012	S1-E1 (331 m)	2005 Oct 27	4
				2006 Aug 14	5
217014	51 Peg A	218261	S1-E1 (331 m)	2006 Aug 12	7

Note.—Observations for HD 189733 were obtained using the H band, while all other observations were obtained using the K' band.

in visible wavelengths (Berger et al. 2006). For barely resolved calibrators, this effect is negligible.

In an effort to find reliable calibrators, we made spectral energy distribution (SED) fits based on published *UBVRIJHK* photometric values for each calibrator to establish diameter estimates and to check if there was any excess emission associated with a low-mass stellar companion or circumstellar disk. Calibrator candidates with variable radial velocities reported in the literature or with any other indication of a possible companion were discarded even if their SEDs displayed no characteristics of duality

TABLE 2
CALIBRATOR STARS' BASIC PARAMETERS

HD	$T_{\rm eff}$ (K)	log g	$\theta_{\rm LD}$ (mas)	Reference
4568	6310	3.95	0.347 ± 0.006	1
6920	6026	3.67	0.543 ± 0.028	1
10477	4800	2.24	0.439 ± 0.018	2
11007	6165	4.20	0.511 ± 0.025	1
13456	6760	4.00	0.380 ± 0.011	1
19411	5050	2.54	0.485 ± 0.019	2
21864	4660	2.14	0.440 ± 0.018	2
22521	5783	3.96	0.377 ± 0.008	3
43318	6456	4.01	0.491 ± 0.030	1
49736	6026	4.25	0.312 ± 0.006	1
61630	4400	1.94	1.116 ± 0.067	2
72779	5790	2.90	0.413 ± 0.010	4
97619	4390	1.94	0.835 ± 0.083	2
121107	5450	1.74	0.686 ± 0.013	2
136849	10741	4.24	0.255 ± 0.016	1
151044	6166	4.38	0.379 ± 0.012	1
176377	5888	4.47	0.358 ± 0.007	1
184960	6456	4.33	0.489 ± 0.017	1
189108	4800	2.34	0.585 ± 0.051	2
190470	4968	4.50	0.340 ± 0.009	5
190993	19055	...	0.167 ± 0.035	6
194012	6309	4.36	0.412 ± 0.008	1
218261	6165	4.40	0.384 ± 0.015	1

REFERENCES.—Sources of the $T_{\rm eff}$ and log g values. (1) Allende Prieto & Lambert 1999; (2) Cox 2000. $T_{\rm eff}$ and log g based on spectral type as listed in the *SIMBAD Astronomical Database*; (3) Soubiran & Girard 2005; (4) Gray et al. 2001; (5) Gray et al. 2003; (6) Baines et al. 2007.

Limb-darkened angular diameter estimates for the calibrators were determined using Kurucz model atmospheres[3] based on $T_{\rm eff}$ and log g values obtained from the literature. The models were then fit to observed photometric values also from the literature, after converting magnitudes to fluxes using Colina et al. (1996) for *UBVRI* values and Cohen et al. (2003) for *JHK* values. See Table 2 for the $T_{\rm eff}$ and log g used and the resulting limb-darkened angular diameters.

Table 3 lists the Modified Julian Date (MJD), baseline (B), position angle (Θ), calibrated visibility (V_c), and error in V_c (σ_{Vc}) for each exoplanet host star observed. It shows the information for one star here as an example; the full table is available on the electronic version of the *Astrophysical Journal*.

[3] Available to download at http://kurucz.cfa.harvard.edu.

TABLE 3
EXOPLANET HOST STARS' CALIBRATED VISIBILITIES

Target Name	MJD	Baseline (m)	Θ (deg)	V_c	σV_c
HD 3651	53665.387	311.95	174.5	0.621	0.072
	53665.400	312.97	171.3	0.647	0.059
	53667.328	312.67	187.9	0.703	0.041
	53667.347	311.52	183.3	0.723	0.059
	53667.364	311.29	179.0	0.676	0.046
	53667.377	311.69	175.7	0.713	0.072
	53667.390	312.53	172.5	0.653	0.053
	53667.402	313.79	169.4	0.590	0.063

NOTES.—The position angle (Θ) is calculated to be east of north. Table 3 is published in its entirety in the electronic edition of the *Astrophysical Journal*. A portion is shown here for guidance regarding its form and content.

TABLE 4
PHOTOMETRIC SOURCES

HD	U	B	V	R	I
3651	1	1	1	1	1
9826	1	1	1	1	1
10697	...	2	2	3	3
11964	...	2	2	3	3
13189	...	2	2	3	3
19994	4	4	4	3	3
20367	...	2	2	3	3
23596	...	2	2	3	3
38529	...	2	2	3	3
50554	...	2	2	3	3
59686	...	2	2	3	3
75732	...	2	2	3	3
104985	4	4	4	3	3
117176	1	1	1	1	1
120136	1	1	1	1	1
143761	4	4	4	3	3
145675	...	2	2	3	3
177830	5	5	5	3	3
186427	4	4	4	3	3
189733	...	2	2	3	3
190228	6	6	6	3	3
190360	4	4	4	3	3
196885	...	2	2	3	3
217014	1	1	1	1	1

NOTES.—All *JHK* photometry from Cutri et al. (2003). Sources: (1) Morel & Magnenat 1978; (2) Perryman & ESA 1997; (3) Monet et al. 2003; (4) Johnson et al. 1966; (5) Mermilliod 1991 (VizieR Online Data Catalog, II/168); (6) Myers et al. 2002 (VizieR Online Data Catalog V/109).

3. ANGULAR DIAMETER DETERMINATIONS

The observed quantity of an interferometer is defined as the squared visibility, although we use the unsquared visibility (V) in our calculations here. Diameter fits to visibilities were based on the uniform disk (UD) approximation given by

$$V = \frac{2J_1(x)}{x}, \tag{1}$$

where J_1 is the first-order Bessel function and

$$x = \pi B \theta_{\rm UD} \lambda^{-1}, \tag{2}$$

where B is the projected baseline at the star's position, $\theta_{\rm UD}$ is the apparent UD angular diameter of the star, and λ is the effective wavelength of the observation[4] (Shao & Colavita 1992). The limb-darkened (LD) relationship incorporating the linear limb darkening coefficient μ_λ (Hanbury-Brown et al. 1974) is given by

$$V = \left(\frac{1-\mu_\lambda}{2} + \frac{\mu_\lambda}{3}\right)^{-1} \times \left[(1-\mu_\lambda)\frac{J_1(x)}{x} + \mu_\lambda \left(\frac{\pi}{2}\right)^{1/2} \frac{J_{3/2}(x)}{x^{3/2}}\right]. \tag{3}$$

[4] Because the flux distributions for these stars in the K' band are in the Rayleigh-Jeans tail, there are no significant differences in the effective wavelengths for stars of differing spectral types.

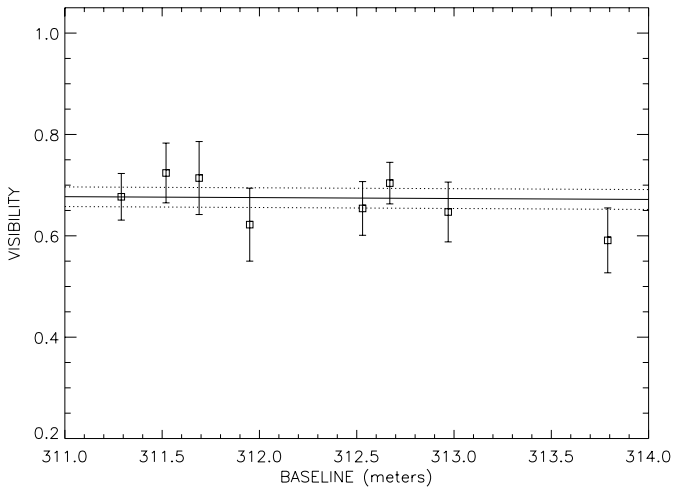

FIG. 1.—Limb-darkened disk diameter fits, showing calibrated visibility vs. baseline. The solid line represents the theoretical visibility curve for a star with the best-fit θ_{LD}, the dashed lines are the 1 σ error limits of the diameter fit, the squares are the calibrated visibilities, and the vertical lines are the measured errors. [*See the electronic edition of the Journal for additional panels of this figure showing all 24 objects*.]

The limb-darkening coefficient was obtained from Claret et al. (1995) after adopting the T_{eff} and log g values required for each star observed. The resulting angular diameters and other relevant parameters are listed in Table 4. The average difference between the UD and LD diameters are on the order of a few percent, and the final angular diameters are little affected by the choice of μ_λ. A 20% change in μ_λ produced at most a 0.6% difference in the angular diameter calculation, so even if the T_{eff} and log g are not well constrained and therefore μ_λ is not precisely known, the effect on the LD diameter (θ_{LD}) will not be significant. Figure 1 shows an example of a diameter fit to calibrated visibilities; additional panels showing all 24 objects are available in the electronic edition of the *Journal*.

It was assumed that the visibility curve went to unity at a baseline of 0 m, and this carried certain implications. For instance, it was assumed the exoplanet host star was a single star and did not host an unseen stellar companion. A companion check was performed for the stars by studying any possible systematics in the single-star uniform-disk fit errors and by searching for separated fringe packets (Farrington & McAlister 2006), and the stars all appeared to be single. Another assumption was that the calibrator star's angular diameter was known and could be used to calibrate the target star's visibilities. If the calibrated visibilities exceeded 1 for a given data set, that calibrator was discarded and the target star was observed again with a new calibrator.

For each θ_{LD} fit, the errors were derived via the reduced χ^2 minimization method: the diameter fit with the lowest χ^2 was found and the corresponding diameter was the final θ_{LD} for the

TABLE 5
EXOPLANET HOST STAR ANGULAR DIAMETER MEASUREMENTS

HD	Spectral Type	T_{eff} (K)	log g	μ_λ	π (mas)	θ_{SED} (mas)	θ_{UD} (mas)	θ_{LD} (mas)	σ_{LD} (%)	R_{linear} ($R_\odot$)	σ_R (%)	$R_{standard}$ ($R_\odot$)
3651.....	K0 V	5173	4.37	0.28	90.43 ± 0.32	0.767 ± 0.078	0.773 ± 0.026	0.790 ± 0.027	3	0.947 ± 0.032	3	0.85
9826.....	F8 V	6212	4.26	0.24	74.14 ± 0.19	1.095 ± 0.032	1.091 ± 0.009	1.114 ± 0.009	1	1.631 ± 0.014	1	1.2
10697.....	G5 IV	5641	4.05	0.28	30.69 ± 0.43	0.496 ± 0.015	0.475 ± 0.046	0.485 ± 0.046	9	1.72 ± 0.17	10	0.92
11964.....	G5	5248[a]	3.82[a]	0.30	30.43 ± 0.60	0.553 ± 0.013	0.597 ± 0.078	0.611 ± 0.081	13	2.18 ± 0.29	13	0.92
13189.....	K2 II	4050[b]	1.74[b]	0.37	1.80 ± 0.73	0.783 ± 0.043	0.811 ± 0.027	0.836 ± 0.028	3	50.39 ± 20.51	41	~20
19994.....	F8 V	6217	4.29	0.24	44.28 ± 0.28	0.693 ± 0.025	0.774 ± 0.026	0.788 ± 0.026	3	1.930 ± 0.067	3	1.2
20367.....	G0 V	6138	4.53	0.25	37.48 ± 0.63	0.386 ± 0.014	0.400 ± 0.107	0.408 ± 0.109	27	1.18 ± 0.32	27	1.1
23596.....	F8	6108	4.25	0.25	19.84 ± 0.49	0.264 ± 0.008	0.374 ± 0.043	0.381 ± 0.044	12	2.09 ± 0.24	12	1.2
38529.....	G4 IV	5674	3.94	0.28	25.46 ± 0.40	0.570 ± 0.028	0.561 ± 0.048	0.573 ± 0.049	9	2.44 ± 0.22	9	1.1
50554.....	F8	6026	4.41	0.26	33.44 ± 0.59	0.326 ± 0.009	0.338 ± 0.098	0.344 ± 0.100	29	1.11 ± 0.33	29	1.2
59686.....	K2 III	4571[a]	2.40[a]	0.34	10.33 ± 0.28	1.287 ± 0.064	1.074 ± 0.011	1.106 ± 0.011	1	11.62 ± 0.34	3	~20
75732.....	G8 V	5279	4.37	0.30	80.55 ± 0.70	0.666 ± 0.029	0.834 ± 0.024	0.854 ± 0.024	3	1.150 ± 0.035	3	0.90
104985.....	G9 III	4877[c]	2.85[c]	0.31	10.30 ± 0.25	0.955 ± 0.065	1.006 ± 0.022	1.032 ± 0.023	2	10.87 ± 0.36	3	~14
117176.....	G4 V	5560	4.07	0.28	55.59 ± 0.24	0.951 ± 0.068	0.986 ± 0.023	1.009 ± 0.024	2	1.968 ± 0.047	2	0.92
120136.....	F7 V	6339	4.19	0.24	64.03 ± 0.20	0.853 ± 0.037	0.771 ± 0.015	0.786 ± 0.016	2	1.331 ± 0.027	2	1.3
143761.....	G0 V	5853	4.41	0.26	58.02 ± 0.28	0.700 ± 0.049	0.673 ± 0.043	0.686 ± 0.044	6	1.284 ± 0.082	6	1.1
145675.....	K0 V	5311	4.42	0.30	56.89 ± 0.35	0.498 ± 0.008	0.363 ± 0.043	0.371 ± 0.044	12	0.708 ± 0.085	12	0.85
177830.....	K0 IV	4804	3.57	0.33	16.94 ± 0.63	0.515 ± 0.023	0.455 ± 0.057	0.467 ± 0.058	12	2.99 ± 0.39	13	0.85
186427.....	G2.5 V	5772	4.40	0.27	47.13 ± 0.27	0.494 ± 0.019	0.417 ± 0.055	0.426 ± 0.056	13	0.98 ± 0.13	13	1.0
189733.....	K1 V	5051[d]	4.53[d]	0.36	51.40 ± 0.69	0.363 ± 0.011	0.366 ± 0.024	0.377 ± 0.024	6	0.788 ± 0.051	7	0.80
190228.....	G5 IV	5312	3.87	0.30	16.25 ± 0.64	0.375 ± 0.032	0.443 ± 0.045	0.453 ± 0.046	10	3.02 ± 0.33	11	0.92
190360.....	G6 IV	5584	4.37	0.28	63.07 ± 0.34	0.658 ± 0.031	0.682 ± 0.019	0.698 ± 0.019	3	1.200 ± 0.033	3	0.92
196885.....	F8 IV	6310[a]	4.32[a]	0.24	29.83 ± 0.48	0.365 ± 0.016	0.485 ± 0.046	0.494 ± 0.046	9	1.79 ± 0.17	10	1.2
217014.....	G2–3 V	5804	4.42	0.27	64.09 ± 0.38	0.665 ± 0.047	0.733 ± 0.026	0.748 ± 0.027	4	1.266 ± 0.046	4	1.0

NOTES.—All T_{eff} and log g are from Santos et al. (2004) unless otherwise noted as from (a) Allende Prieto & Lambert (1999); (b) Cox (2000); (c) Takeda et al. (2005); (d) Sousa et al. (2006). The μ_λ values are from Claret et al. (1995), and π values are from van Leeuwen (2007). The spectral classes are from the following sources: HD 3651: Fischer et al. (2003); HD 9826: Butler et al. (1999); HD 10697: Vogt et al. (2000); HD 11964: Butler et al. (2006); HD 19994: Mayor et al. (2004); HD 20367: Butler et al. (2006) ; HD 23596: Valenti & Fischer (2005); HD 38526: Fischer et al. (2001); HD 50554: Perrier et al. (2003); HD 59686: Cox (2000); HD 75732: Marcy et al. (2002); HD 104985: Sato et al. (2003); HD 117176: Marcy & Butler (1996); HD 120136: Butler et al. (1997); HD 143761: Noyes et al. (1997); HD 145675: Butler et al. (2003); HD 177830: Vogt et al. (2000); HD 186427: Cochran et al. (1997); HD 189733: Bouchy et al. (2005); HD 190228: Perrier et al. (2003); HD 190360: Naef et al. (2003); HD 196885: Jones et al. (2006); and HD 217014: Marcy et al. (1997).

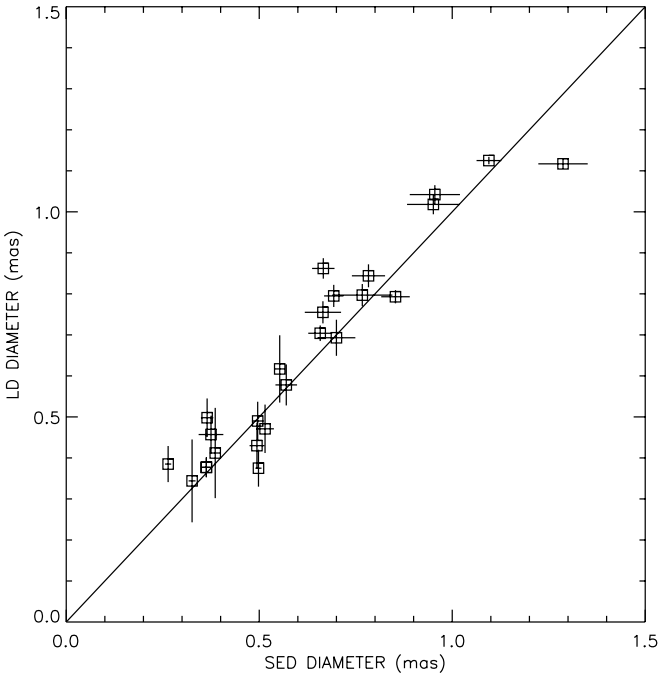

FIG. 2.— Comparison of estimated SED diameters and measured LD diameters. The solid line indicates a 1:1 ratio for the diameters. Note that at $\theta > 0.6$ mas, the errors for the measured LD diameters become equal to or smaller than the errors from the SED diameter estimates.

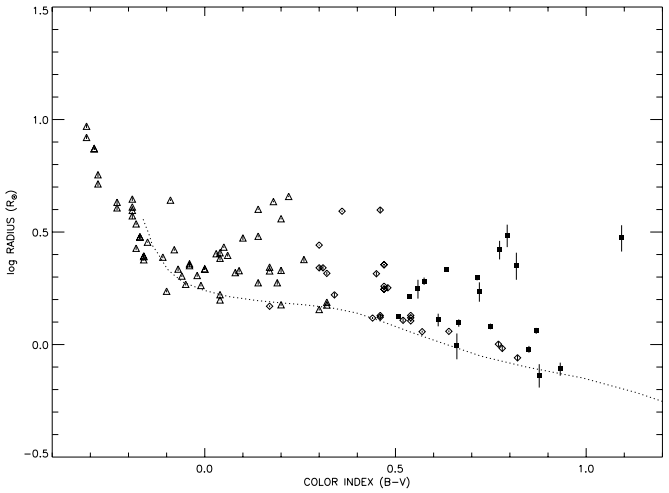

FIG. 3.—Stellar radii: log R vs. unreddened color index ($B - V$). The triangles represent O, B, and A dwarf stars from the Andersen sample (Andersen 1991); diamonds represent F, G, and K dwarf stars from the Andersen sample; and the filled squares represent exoplanet host stars' diameters measured here with errors <15%. The dotted line indicates the ZAMS for stars with masses between 0.15 and 5.0 $M_\odot$ (Girardi et al. 2000).

star. The errors were calculated by finding the diameter at $\chi^2 + 1$ on either side of the minimum χ^2 and determining the difference between the χ^2 diameter and $\chi^2 + 1$ diameter.

Table 4 lists the parameters $T_{\rm eff}$ and log g from spectroscopic studies that define the limb-darkening coefficient μ_λ. The $\theta_{\rm UD}$ was converted to $\theta_{\rm LD}$ using μ_λ, and the combination of $\theta_{\rm LD}$ and the *Hipparcos* parallax (van Leeuwen 2007) led to a linear radius for the star. Table 4 also includes LD diameters estimated from SED fits ($\theta_{\rm SED}$) as a comparison to the measured diameters. The sources for the photometry used are listed in Table 5 and are available online. The term $R_{\rm standard}$ represents the radius expected from the spectral type listed in the second column.

3.1. *Estimated vs. Measured Stellar Diameters*

To check the correspondence between the estimated and measured diameters, Figure 2 plots $\theta_{\rm LD}$ versus $\theta_{\rm SED}$. At diameters $\gtrsim$0.6 mas, the errors for $\theta_{\rm LD}$ become smaller than those for $\theta_{\rm SED}$. This is to be expected, as the smaller diameters are nearing the resolution limit of the CHARA Array, and the uncertainties will be larger for these measurements.

In order to characterize the scatter in the diameters, the standard deviation σ of the quantity $(\theta_{\rm LD} - \theta_{\rm SED})$ was determined and was then divided by $\theta_{\rm SED}$ for each star. Then all the $\sigma/\theta_{\rm SED}$ were averaged together, with a resulting value of 12%. This indicates a fairly good correspondence between the estimated and measured diameters.

4. COMBINING STELLAR RADII FROM INTERFEROMETRY AND ECLIPSING BINARY SYSTEMS

It was of particular interest to combine interferometrically measured stellar radii and radii determined using other direct means in order to check their compatibility. Some of the most precise stellar radii result from measuring detached, double-lined eclipsing binary systems, as described in Andersen (1991). His sample encompasses all spectral types from O8 V to M1 V, and includes one system of two evolved stars. The errors in the radius measurements are $\leq$2%, and the values are presumed to be valid for single stars.

Figure 3 shows the stellar radii measured from eclipsing binaries and the exoplanet host stars' linear radii measured here with errors <15%. The Andersen sample has few G and K dwarfs, and our work helps better populate the low-mass range by tripling the number of stellar radii measurements in the $0.5 \leq (B - V) \leq 1.0$ portion of the plot. The radii measured from eclipsing binaries support the validity of the interferometric measurements. Although 21 stars measured here have linear radii errors <15%, 19 are shown in Figure 3. The remaining targets are HD 59686, a K2 III star, and HD 104985, a G9 III star. The figure demonstrates that many stars in our and the Andersen sample are post–zero-age main-sequence (ZAMS) objects.

4.1. *Separating Dwarfs and Subgiants*

Interferometrically derived radii may reveal the beginnings of post-main-sequence evolution for stars previously classified as dwarfs. Figure 4 plots the stars listed in Table 4 on a color-magnitude plot, except for the giants in the sample (HD 13189, HD 59686, and HD 104985). Over half the stars lie on a fairly well-defined main sequence (MS), and their measured radii generally match the expected values (see Fig. 4). Because there will be some spread in the MS due to stars having a nonzero age, we concentrate on the more evolved cases below.

Five of the stars were previously classified as subgiants and, as expected, lie well off the MS. HD 10697, HD 38529, HD 177830, and HD 190228 were labeled as subgiants by the papers listed in Table 4, and observations confirm the classification. The fifth star, HD 11964, was given a G5 spectral type with no luminosity class. Its measured radius is over twice that expected for a G5 dwarf, and so is most likely a subgiant.

Another group of stars previously classified as dwarfs show measured radii that substantially exceed what is expected from the stars' spectral types as given by Cox (2000), and show indications of post MS evolution. These stars are:

HD 19994.—Mayor et al. (2004) classified this star as an F8 V star when the planetary system was discovered. Its measured

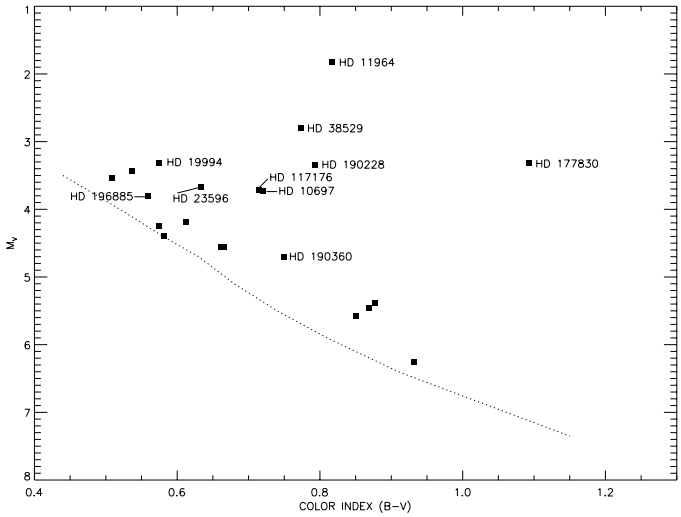

FIG. 4.—Absolute V magnitude vs. color index ($B - V$). The dotted line indicates the ZAMS derived from Cox (2000). The unlabeled points are dwarfs with no problems in their measured radii. HD 10697, HD 11964, HD 38529, HD 177830, and HD 190228 are confirmed subgiants, while HD 19994 and HD 117176 are stars showing signs of post-MS evolution. See § 4.1 for details on these stars and on HD 23596, HD 190360, and HD 196885.

radius is ∼60% larger than that expected for a standard F8 dwarf star.

HD 23596.—No luminosity class was assigned to HD 23596 by the SIMBAD Astronomical Database, only a spectral type of F8. Its measured radius is ∼75% larger than that of an F8 dwarf.

HD 117176.—Marcy & Butler (1996) labeled this star as G4 V, and the associated radius for that spectral classification is 0.92 $R_\odot$. However, the measured radius is well over twice that value, and it is placed next to HD 10697, a known subgiant, on the color-magnitude diagram.

HD 190360.—Naef et al. (2003) classified HD 190360 as a G6 IV star, and our radius measurement is ∼30% larger than that of a G6 V star. While the star shows no photometric indication of significant evolution off the MS, the radius measurement is overlarge for a dwarf.

HD 196885.—This star was labeled as an F8 IV by Jones et al. (2006), and its measured radius exceeds the expected radius for an F8 V by ∼50%. Although there is no photometric evidence of evolution, its radius is significantly larger than expected if the star was a dwarf.

5. CONCLUSION

We observed 24 exoplanet systems in order to measure the host stars' diameters, obtaining 22 limb-darkened angular diameters with errors <15%. After the LD diameters were converted to linear radii when combined with *Hipparcos* parallax, 19 dwarf stars boasted radius errors of <15%, and these were plotted with the radii from the eclipsing binary sample from Andersen (1991). These new results tripled the number of stars in the $0.5 \leq (B - V) \leq 1.0$ range with known radii. Three giants, 5 subgiants, 11 dwarfs, and 5 moderately evolved stars were measured, covering a wide range of evolutionary stages.

Many thanks to Chris Farrington for his invaluable assistance in obtaining some of the data used here. The CHARA Array is funded by the National Science Foundation through NSF grants AST-0307562 and AST-0606958 and by Georgia State University through the College of Arts and Sciences and the Office of the Vice President for Research. This research has made use of the SIMBAD literature database, operated at CDS, Strasbourg, France, and of NASA's Astrophysics Data System. This publication makes use of data products from the Two Micron All Sky Survey, which is a joint project of the University of Massachusetts and the Infrared Processing and Analysis Center/California Institute of Technology, funded by the National Aeronautics and Space Administration and the National Science Foundation.

REFERENCES

Allende Prieto, C., & Lambert, D. L. 1999, A&A, 352, 555
Andersen, J. 1991, Astron. Astrophys. Rev., 3, 91
Baines, E. K., et al. 2007, ApJ, 661, L195
Berger, D. H., et al. 2006, ApJ, 644, 475
Bouchy, F., et al. 2005, A&A, 444, L15
Butler, R. P., et al. 1997, ApJ, 474, L115
———. 1999, ApJ, 526, 916
———. 2003, ApJ, 582, 455
———. 2006, ApJ, 646, 505
Claret, A., Diaz-Cordoves, J., & Gimenez, A. 1995, A&AS, 114, 247
Cochran, W. D., et al. 1997, ApJ, 483, 457
Cohen, M., Wheaton, W. A., & Megeath, S. T. 2003, AJ, 126, 1090
Colina, L., Bohlin, R. C., & Castelli, F. 1996, AJ, 112, 307
Cox, A. N. 2000, Allen's Astrophysical Quantities, 4th ed., ed. A. N. Cox (New York: AIP)
Cutri, R. M., et al. 2003, The IRSA 2MASS All-Sky Point Source Catalog (NASA/IPAC Infrared Science Archive), http://irsa.ipac.caltech.edu/applications/Gator/
Farrington, C. D., & McAlister, H. A. 2006, Proc. SPIE, 6268, 1
Fischer, D. A., & Valenti, J. 2005, ApJ, 622, 1102
Fischer, D. A., et al. 2001, ApJ, 551, 1107
———. 2003, ApJ, 590, 1081
Girardi, L., Bressan, A., Bertelli, G., & Chiosi, C. 2000, A&AS, 141, 371
Gray, R. O., Corbally, C. J., Garrison, R. F., McFadden, M. T., & Robinson, P. E. 2003, AJ, 126, 2048
Gray, R. O., Graham, P. W., & Hoyt, S. R. 2001, AJ, 121, 2159
Hanbury-Brown, R., et al. 1974, MNRAS, 167, 475
Johnson, H. L., Iriarte, B., Mitchell, R. I., & Wisniewskj, W. Z. 1966, Commun. Lunar Planet. Lab., 4, 99
Jones, B. W., Sleep, P. N., & Underwood, D. R. 2006, ApJ, 649, 1010
Marcy, G. W., & Butler, R. P. 1996, ApJ, 464, L147
Marcy, G. W., et al. 1997, ApJ, 481, 926
———. 2002, ApJ, 581, 1375
———. 2005, ApJ, 619, 570
Mayor, M., et al. 2004, A&A, 415, 391
McAlister, H. A., et al. 2005, ApJ, 628, 439
Mermilliod, J. C. 1991, Catalogue of Homogeneous Means in the UBV System (Lausane: Univ. de Lausanne)
Monet, D. G., et al. 2003, AJ, 125, 984
Morel, M., & Magnenat, P. 1978, A&AS, 34, 477
Myers, J. R., et al. 2002, SKY2000 Catalog, Ver. 4 (NASA: GSFC)
Naef, D., et al. 2003, A&A, 410, 1051
Noyes, R. W., et al. 1997, ApJ, 483, L111
Perrier, C., et al. 2003, A&A, 410, 1039
Perryman, M. A. C., & ESA. 1997, The *Hipparcos* and TYCHO Catalogues (ESA SP-1200; Noordwijk: ESA)
Ribas, et al. 2003, A&A, 411, L501
Santos, N. C., Israelian, G., & Mayor, M. 2004, A&A, 415, 1153
Sato, B., et al. 2003, ApJ, 597, L157
Shao, M., & Colavita, M. M. 1992, ARA&A, 30, 457
Soubiran, C., & Girard, P. 2005, A&A, 438, 139
Sousa, S. G., et al. 2006, A&A, 458, 873
Takeda, Y., et al. 2005, PASJ, 57, 109
ten Brummelaar, T. A., et al. 2005, ApJ, 628, 453
Valenti, J. A., & Fischer, D. A. 2005, ApJS, 159, 141
van Leeuwen, F. 2007, *Hipparcos*, the New Reduction of the Raw Data (Berlin: Springer)